水路部研究報告　第38号　平成14年3月30日
REPORT OF HYDROGRAPHIC RESEARCHES No.38 March, 2002

Improved Co-tidal Charts around Osaka Bay, Seto Inland Sea. - Influence of Coriolis force on the tidal distribution -†

Minoru ODAMAKI*

Abstract

Using the equation of motion for tide and tidal current around Osaka Bay, momentum balance of tidal waves are investigated and precise co-tidal charts are edited. Some distinctive characteristics are recognized in the charts such as nodal area of M_2 tide shifted to the northern corner of Awaji-shima. These distributions are almost explained by the influence of Coriolis force on tidal current. In addition, generation of shallow water tide of M_4 around Akashi-strait, which was first introduced by S. Ogura(1933), is quantitatively discussed based on tidal current data.

1．Introduction

Osaka Bay is a semi-enclosed bay located in the eastern end of the Seto Inland Sea and communicates with Kii-channel and Harima-nada through Tomogashima- and Akashi-straits as shown in Fig. 1. Around the latter strait, there is unique sea bottom topography such as caldrons and sand waves, concerned to erosion, transport and sedimentation by tidal current (Yashima 1992). Thus tide and tidal current are basically important for marine environment in this area, and they show unique phenomena in physical oceanography, too. For example, a node of semidiurnal tide appears in Akashi-strait (Ogura 1933a), where its amplitude becomes in minimum. In contrary, tidal current is developed intensively and its speed reaches about 7 knots in maximum. Further, shallow water tides are developed in the bay and the straits, which may be induced by this strong semidiurnal current. Ogura (1933a) investigated these features of node and shallow water tides based on the tidal harmonic constants but could not use tidal current observation data.

Therefore, using, tide and tidal current data collected in the Hydrographic Department of Japan, tidal oscillations around Osaka Bay are re-investigated in this paper. Applying the equation of motion in hydrodynamics to the tidal current data, directions of co-tidal and co-amplitude lines are obtained in each observation site as explained in the section 3. Using its results, co-tidal charts in this area are revised and described in the section 4. Tidal wave characteristics are discussed in the section 5.1 focussing the momentum balances and the relation of tide and tidal current in the straits. Particularly, the influence of earth rotation, i.e., Coriolis effect is pointed out, to be indispensable for tides even in the shallow and narrow seas like Osaka Bay. In addition, generation of shallow water tide M_4 is quantitatively discussed in the section 5.2, using the Bernoulli equation and the curved stream effect of tidal current. In the section 6, the results and future subjects are summarized.

† Received 2001 December 20th. ; Accepted 2002 February 5th.
* 海洋研究室 Ocean Research Laboratory.

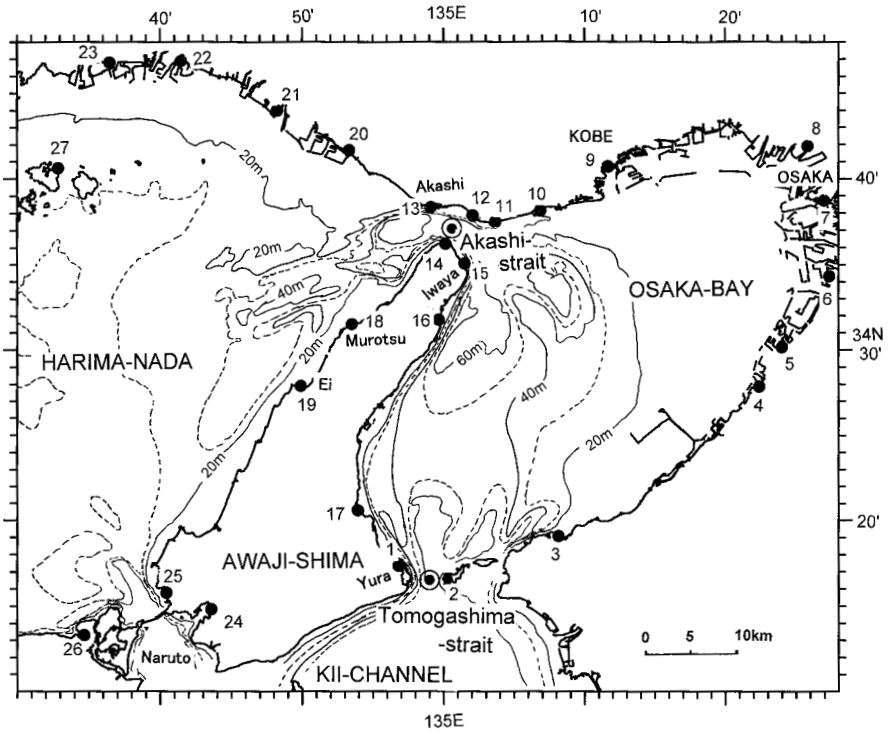

Fig. 1 Location Map of tidal stations.

2. Data source

Tidal harmonic constants in this paper are listed in Table 1, which are almost referred to the publication, No.742 Tidal Harmonic Constants Tables in Japanese coasts (MSA 1992) and the tidal observation reports of the Hydrographic Department and the 5th Regional Japan Coast Guards Headquarters. For some ports, harmonic constants were newly calculated.

Tidal current harmonic constants at 55 stations used for the following analysis are taken from the data collected in the Coastal Surveys and Cartography Division of the Hydrographic Department, and from some tidal current observation reports published by the 5th Reg. JCG Hdqrs. (1996). They are selected from the data observed longer than 15 days to analyze for more than 10 harmonic constituents. For reference, harmonic constants of 4 principal constituents in Akashi- and Tomogashima-straits are listed in Table 2.

In Table 1 and 2, phase lag κ is expressed as lag angle referred to the local transit time in each observation site. For the co-tidal hour referred to Japanese Standard Longitude 135E, the time is adjusted using the formula; Co-tidal hour = (κ + (λ - 135))/ 15n. where, λ is the east longitude and n is tidal species' number, 2 for semidiurnal and 1 for diurnal tide. Denominator 15n means an hour angle of each tidal constituent.

3. Evaluation of co-tidal and co-amplitude lines

Directions of co-tidal and co-amplitude lines at the tidal current station can be evaluated using its harmonic constants and adding tidal harmonic constants (Ogura 1933b, Doodson and Warburg 1950, Odamaki 1989). Assuming advection terms are negligibly small, equation of motion for vertically averaged velocities becomes;

Table 1 Tidal Harmonic Constants around Osaka Bay. Locations of tide stations are shown in Figure 1.

Place	Location	M2		S2		K1		O1		MO3		M4		2MS6		Ref.
		cm	deg.	cm	deg.	cm	deg.	cm	deg.	cm	deg.	cm	deg	cm	deg.	
1 Yura	34° 16'N 134° 57'E	30.6	193.1	16.2	211.0	24.2	206.9	17.8	179.8	0.0	----	0.0	----	0.0		(4)
2 Okinoshima	34° 17'N 135° 01'E	38.8	192.5	19.8	215.4	25.3	201.1	18.7	181.9	----	----	1.8	231.0	----	---	(1)
3 Tannowa	34° 20'N 135° 11'E	32.3	204.2	17.7	221.6	25.2	200.7	19.0	178.8	1.4	304.8	1.2	34.6	1.2	243.9	(1)
4 Kishiwada	34° 28'N 135° 22'E	31.4	211.8	16.7	227.4	26.0	203.7	19.8	180.6	1.7	304.7	1.3	48.5	1.5	267.0	(1)
5 Izumi-Otsu	34° 30'N 135° 24'E	30.4	213.6	17.3	226.4	25.9	203.1	19.2	180.9	2.0	319.8	1.4	44.4	1.8	249.8	(1)
6 Sakai	34° 35'N 135° 28'E	30.6	213.7	17.3	228.4	26.3	202.7	19.7	181.2	1.5	321.4	1.2	50.4	1.6	268.1	(1)
7 Osaka	34° 39'N 135° 26'E	29.9	215.2	16.9	228.2	26.1	203.9	19.8	181.6	1.8	314.6	1.4	38.6	2.0	259.1	(3)
8 Amagasaki	34° 42'N 135° 24'E	30.3	215.7	17.2	229.5	25.9	204.0	19.3	181.8	1.7	316.1	1.3	84.2	2.0	261.5	(1)
9 Kobe	34° 41'N 135° 11'E	28.8	216.3	16.4	228.8	26.0	204.2	19.7	181.8	1.7	311.8	1.3	33.9	1.6	257.8	(3)
10 Suma	34° 38'N 135° 06'E	23.2	224.0	16.0	234.6	24.6	206.5	19.7	179.7	1.1	309.4	1.1	30.2	1.4	259.8	(4)
11 Tarumi	34° 37'N 135° 03'E	26.2	227.5	14.6	234.9	26.7	206.5	20.8	188.6	1.5	281.3	2.9	287.3	0.9	249.0	(4)
12 Maiko	34° 39'N 135° 02'E	24.8	225.6	14.1	231.5	26.8	197.1	16.5	178.8	----	----	4.1	253.1	0.7	218.1	(5)
13 Akashi	34° 38'N 134° 59'E	15.7	243.4	8.5	238.9	26.1	216.7	22.3	191.9	---	-----	1.8	302.5	---	-----	(2)
14 Esaki	34° 36'N 134° 59'E	13.2	239.9	9.4	235.4	25.4	221.7	20.0	202.6	---	-----	5.0	279.5	---	-----	(1)
15 Iwaya	34° 36'N 134° 59'E	16.4	227.5	11.2	231.1	27.7	218.6	22.0	195.2	---	-----	7.6	287.0	---	------	(2)
16 Kariya	34° 31'N 135° 00'E	27.8	204.9	17.7	213.4	25.3	208.2	20.5	184.4	----	----	1.9	21.8	----	---	(1)
17 Sumoto	34° 20'N 134° 55'E	30.5	193.2	17.0	215.0	24.1	204.1	18.4	182.0	1.1	317.4	0.9	48.3	1.0	238.9	(1)
18 Murotsu	34° 32'N 134° 52'E	22.0	335.0	8.0	286.0	26.0	228.0	23.0	206.0	----	----	----	----	----	----	(1)
19 Ei	34° 28'N 134° 49'E	25.0	333.6	5.6	326.0	27.6	230.9	20.4	206.6	----	----	0.8	88.0	----	----	(1)
20 Futami	34° 42'N 134° 54'E	20.4	291.1	7.8	280.5	27.4	223.5	23.0	196.6	----	----	0.9	23.1	----	----	(1)
21 Takasago	34° 44'N 134° 48'E	27.4	313.4	7.7	306.5	27.9	225.9	20.4	200.5	1.2	320.7	1.0	65.2	0.9	142.1	(1)
22 Shikama	34° 47'N 134° 40'E	31.1	315.8	8.7	313.4	28.2	226.0	20.8	202.3	1.1	293.0	1.3	72.0	0.8	129.0	(1)
23 Hirohata	34° 47'N 134° 37'E	33.0	322.6	7.0	311.5	28.0	226.2	23.0	207.1	----	----	----	-----	----	-----	(1)
24 Fukura	34° 15'N 134° 43'E	44.8	191.0	20.9	213.1	23.0	195.5	18.6	26.0	0.5	230.4	0.4	230.0	1.9	148.4	(4)
25 Anaga-Ura	34° 16'N 134° 40'E	32.4	340.6	7.8	351.5	29.1	231.4	21.7	204.1	1.1	309.4	1.1	30.2	1.4	259.8	(1)
26 Kitadomari	34° 14'N 134° 35'E	17.0	277.0	8.7	263.5	25.5	216.7	19.1	191.5	0.6	278.2	1.4	201.5	1.4	164.1	(1)
27 Ie-shima	34° 41'N 134° 32'E	31.2	318.8	8.6	318.2	28.2	226.6	20.6	200.7	----	----	1.2	85.8	----	----	(1)

(1) Tidal Harmonic Constant Table(1992), (2)Hiraiwa et al.(1996), (3) from Tidal Data Base of Head Office,
(4) New calculation using tidal data by 5th regional office, (5) New calculation but data length is short, only 7days.

$$(1)\quad \begin{cases} \dfrac{\partial u}{\partial t} - fv = -g\dfrac{\partial \eta}{\partial x} - \dfrac{1}{h}\tau_{bx} \\ \dfrac{\partial v}{\partial t} + fu = -g\dfrac{\partial \eta}{\partial y} - \dfrac{1}{h}\tau_{by} \end{cases}$$

where u is horizontal velocity of x-axis, v: that of y-axis, f: Coriolis coefficient, g: gravity acceleration, η: sea surface elevation, τ_b: bottom stress. Applying tidal oscillation of frequency σ, time variables are expressed as $u = \mathrm{U}\cos(\sigma t - \kappa_u) = U_C cos(\sigma t) + U_S sin(\sigma t)$, [$U_C = \mathrm{U} cos(\kappa_u)$, $U_S = \mathrm{U} sin(\kappa_u)$], $\eta = \mathrm{H}cos(\sigma t - \kappa) = H_C\ cos(\sigma t) + H_S\ sin(\sigma t)$, [$H_C = \mathrm{H}cos(\kappa)$, $H_S = \mathrm{H}sin(\kappa)$], and so on. Bottom stresses are also expressed as *sin* and *cos* components, as explained in the last of this section.

Considering separation of *cos* and *sin* function, each equation becomes;

$$(2)\quad \begin{cases} -\sigma U_C - fV_S = -g\dfrac{\partial}{\partial x}H_S - \dfrac{1}{h}\tau_{bxs} \\ \sigma U_S - fV_C = -g\dfrac{\partial}{\partial x}H_C - \dfrac{1}{h}\tau_{bxc} \\ -\sigma V_C + fU_S = -g\dfrac{\partial}{\partial y}H_S - \dfrac{1}{h}\tau_{bys} \\ \sigma V_S + fU_C = -g\dfrac{\partial}{\partial y}H_C - \dfrac{1}{h}\tau_{byc} \end{cases}$$

(a) (b) (c) (d)

where (a) indicates time variable, (b) Coriolis, (c) pressure gradient, and (d) bottom stress terms.

Transferring terms, we can get the gradients of *cos* and *sin* components of elevation,

$$(3)\quad \begin{cases} \dfrac{\partial H_S}{\partial x} = \dfrac{1}{g}\left\{\sigma U_C + fV_S - \dfrac{1}{h}\tau_{bxs}\right\} \\ \dfrac{\partial H_C}{\partial x} = \dfrac{1}{g}\left\{-\sigma U_S + fV_C - \dfrac{1}{h}\tau_{bxc}\right\} \\ \dfrac{\partial H_S}{\partial y} = \dfrac{1}{g}\left\{\sigma V_C - fU_S - \dfrac{1}{h}\tau_{bys}\right\} \\ \dfrac{\partial H_C}{\partial y} = \dfrac{1}{g}\left\{-\sigma V_S - fU_C - \dfrac{1}{h}\tau_{byc}\right\} \end{cases}$$

Right-hand terms of this equation are known using tidal current harmonic constants.

Besides, horizontal derivatives in x-direction of each component of elevation, H_C and H_S, are expressed by composites of amplitude H and phase lag κ;

$$(4)\quad \begin{cases} \dfrac{\partial H_C}{\partial x} = \dfrac{\partial}{\partial x}(\mathrm{H}cos\kappa) = \dfrac{\partial \mathrm{H}}{\partial x}cos\kappa - \mathrm{H}sin\kappa\dfrac{\partial \kappa}{\partial x} \\ \dfrac{\partial H_S}{\partial x} = \dfrac{\partial}{\partial x}(\mathrm{H}sin\kappa) = \dfrac{\partial \mathrm{H}}{\partial x}sin\kappa + \mathrm{H}cos\kappa\dfrac{\partial \kappa}{\partial x} \end{cases}$$

If x is exchanged with y, derivative for y-direction is obtained.

From this formula (4), horizontal gradients of H and κ are expressed as,

$$(5)\quad \begin{cases} \dfrac{\partial \mathrm{H}}{\partial x} = \dfrac{1}{\mathrm{H}}\left\{H_C\dfrac{\partial H_C}{\partial x} + H_S\dfrac{\partial H_S}{\partial x}\right\} \\ \dfrac{\partial \kappa}{\partial x} = \dfrac{1}{\mathrm{H}^2}\left\{-H_S\dfrac{\partial H_C}{\partial x} + H_C\dfrac{\partial H_S}{\partial x}\right\} \end{cases}$$

Inserting the values of (3) to (5), the horizontal gradients of H and κ, i.e., directions of co-tidal and co-amplitude lines are finally obtained.

Assuming the linearity for brevity according to Unoki (1993), the bottom stress terms are expressed;

$$(6)\quad \begin{cases} \tau_{bx} = \dfrac{8}{3\pi}\gamma_b \cdot \sqrt{\mathrm{U}^2 + \mathrm{V}^2} \cdot u \\ \tau_{by} = \dfrac{8}{3\pi}\gamma_b \cdot \sqrt{\mathrm{U}^2 + \mathrm{V}^2} \cdot v \end{cases}$$

where $8/3\pi$ is the integral coefficient and γ_b is the drag coefficient 0.0026. u and v are velocity components in x and y directions as same as (1), and U and V are their amplitudes respectively.

4. Co-tidal and Co-amplitude charts

Co-tidal and co-amplitude charts of M_2, S_2, K_1, and O_1 are shown in Fig. 2 to 5. Arrow with bar in each chart means direction of increasing

for co-tidal hour or tidal amplitude, which is estimated from tidal current harmonic constants using the equation (5) as mentioned above. Length of arrow indicates magnitude of increasing rate and bar indicates the direction of co-amplitude or co-tidal line.

Naruto-kaikyo is a very narrow strait connecting Kii-channel and Harima-nada. Both sides of Naruto-kaikyo, tides are so different that many co-tidal and co-amplitude lines should be drawn. But tide around Naruto-kaikyo is not discussed in this paper so the lines were not drawn there in the charts.

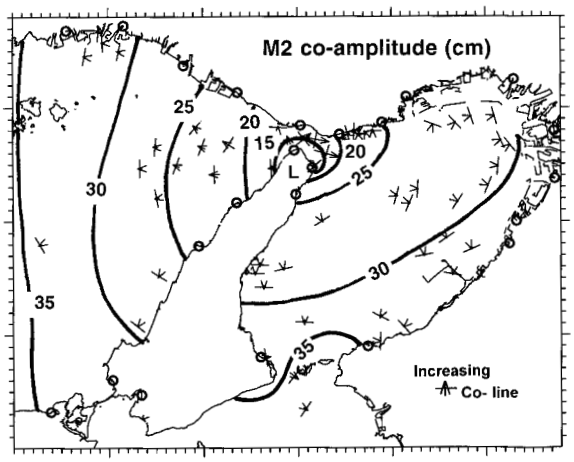

Fig. 2(a) Co-amplitude chart for M_2 tide. Contour interval is 5cm. Arrow with small bar means the direction and magnitude of gradient for M_2 tidal amplitude.

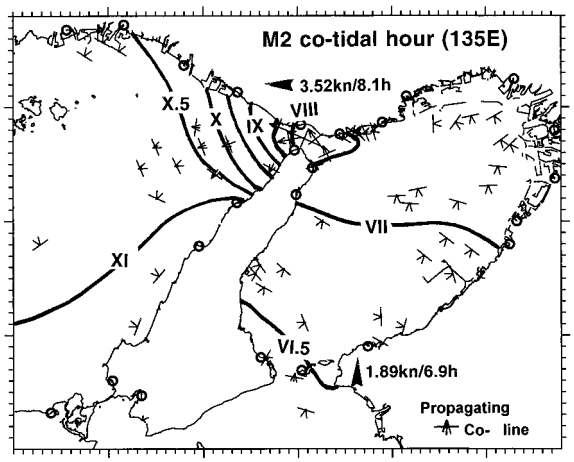

Fig. 2(b) Co-tidal chart for M_2 tide. Roman numeral attached to co-tidal line means the lapse hour (15 degrees per hour) from the transit of M_2 at 135E longitude to High water at the site. Arrow with small bar means the direction and magnitude of gradient for M_2 phase lag.

4. 1 M_2 tide

As shown in the co-amplitude chart of Fig. 2(a), M_2 tidal amplitude is about 35cm in the south of Tomogashima-strait and decreases toward inner side of Osaka Bay. As well known, M_2 tidal amplitude becomes in minimum 15-20 cm in Akashi-strait, and increases 35 cm in the central area of Harima-nada. Then co-amplitude lines expand both sides of Akashi-strait like concentric circles. Particularly, in Akashi-strait tidal amplitude at the southern coast is smaller than that at the northern coast and co-amplitude line of 15cm surrounds the northern corner of Awaji-shima. Thus, tidal amplitude at the right-hand side of propagating direction is larger than that at the left-hand side even in the narrow strait such as Akashi-strait. Similarly, in Tomogashima-strait, M_2 tidal amplitude at the right-hand side, eastern coast, is larger than that at the left-hand side, western coast.

M_2 co-tidal chart of Fig. 2(b) shows the propagation of tidal wave from the south of Tomogashima-strait 6.5 hours through Osaka Bay about 7 hours to Harima-nada about 10.5 to 11 hours. In Akashi-strait, co-tidal lines are gathered closely and its difference of both sides reaches about 3.5 hours. This distribution indicates stationary like a node of standing oscillation. But if a node were physically com-

plete balanced with incident and reflected waves, co-tidal hour would change 6 hours (opposite phase) across the node and would not show propagation. Thereby this co-tidal line distribution can be considered to consist of the incident wave from Osaka Bay principally, and that from Harima-nada subsidiary. As shown in Fig. 2(b), generally, this partial node is not just located at the narrowest of the strait but shifted to the Harima-nada side. Thus co-tidal lines spread along the northeastern coast of Harima-nada and concentrate to Awaji-shima coast. This concentration suggests a virtual amphidromic point located in Awaji-shima as same as in the Irish sea pointed by Hendeshott and Speranza (1971).

Looking into the detail of Fig. 2(a) and 2(b) around Akashi-strait, magnitude of gradient of tidal phase and amplitude become in maximum at the narrowest of the strait where tidal current is almost strongest. But most closely distribution of co-tidal lines is not located there as mentioned above. This discrepancy is considered due to the assumption of neglecting non-linear and horizontal friction terms because the current is flowing into narrow passage and varied in place to place. Furthermore, in general the amplitude decreases to the strait as shown in Fig. 2(a), but in local it increases along the coast from Suma to Tarumi as indicated by the arrows of gradient. This fact is recognized in Table 1 too, in which the amplitude increases from Suma 23.2cm to Tarumi 26.2cm and Maiko 24.8cm. This opposite tendency along the coast is considered due to the counter-current eddy existing there and the assumption of neglecting non-linear terms. As discussed in the later section, in Akashi-strait, M_4 tide caused by non-linear effect is extremely developed. In return, non-linear terms will not be negligible for M2 tide.

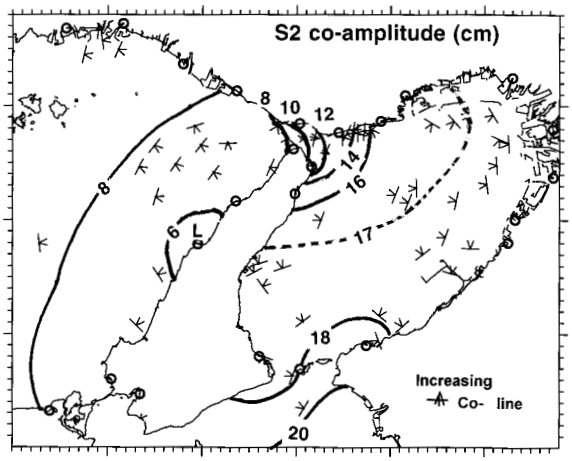

Fig. 3(a) Co-amplitude chart for S_2.

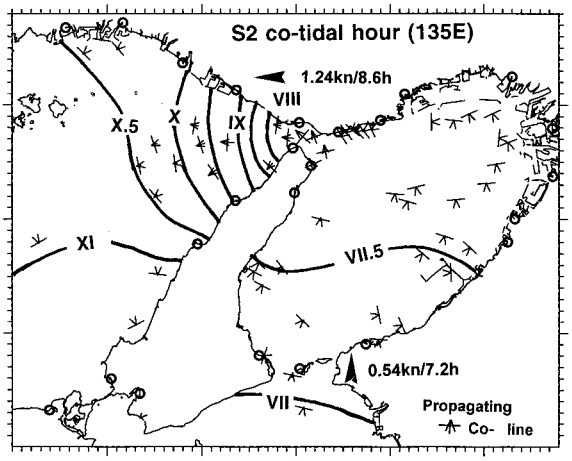

Fig. 3(b) Co-tidal charts for S_2.

4. 2 S_2 tide

Almost same as M_2 tide, S_2 tidal amplitude decreases from the south of Tomogashima-strait to the inner area of Osaka Bay, shown in Fig. 3a. But the amplitude minimum zone is moved from Akashi-strait to the western coast of Awaji-shima around Ei. For M_2 tide, co-amplitude lines are distributed almost symmetrical to Akashi-strait, but for S_2 tide those distribution are asymmetrical because of the west

shift of amplitude minimum zone.

S_2 co-tidal lines also show propagation in Fig. 3(a) from the south of Tomogashima-strait to Harima-nada through Osaka Bay, almost same as those of M_2. But the crowded zone of co-tidal lines are shifted to west from Akashi-strait as same as the amplitude minimum. Further, comparing co-tidal hour between M_2 and S_2, S_2 advances about half-hour to M_2 in Osaka Bay, but is almost same in Harima-nada.

The reason of difference of M_2 and S_2 tidal distribution is considered principally due to the difference of tidal response of the Seto Inland Sea to the tidal inputs of M_2 and S_2 periods. For S_2 tide, its period is 12.00 hours shorter than that of M_2 tide 12.42 hours so that its wave length become shorter than that of M_2. Then S_2 tidal oscillation is realized in shorter scale than that of M_2, and S_2 node is shifted to inner area comparing to M_2.

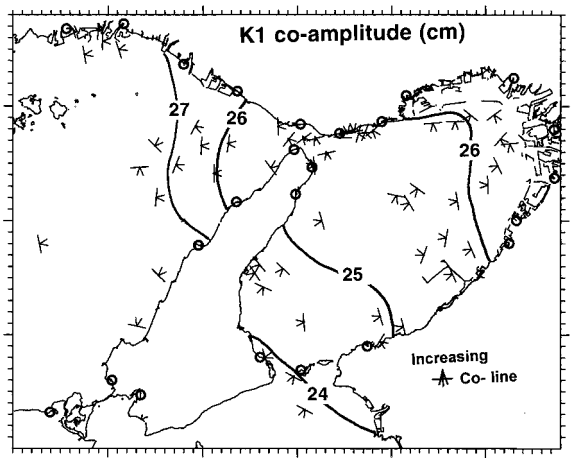

Fig. 4(a) Co-amplitude chart for K_1.

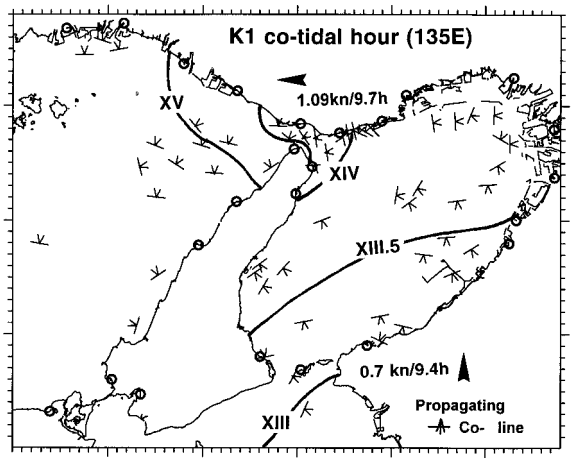

Fig. 4(b) Co-tidal charts for K_1.

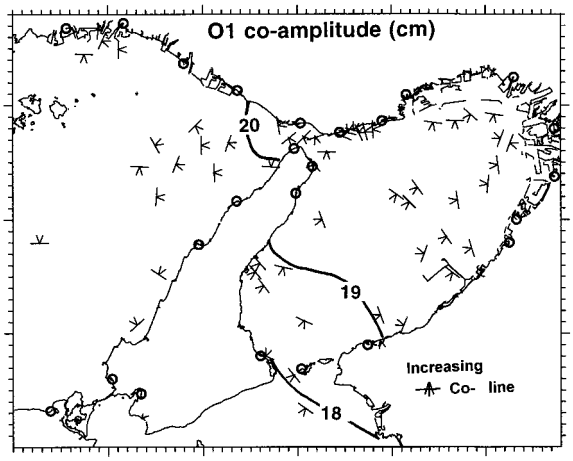

Fig. 5(a) Co-amplitude chart for O_1.

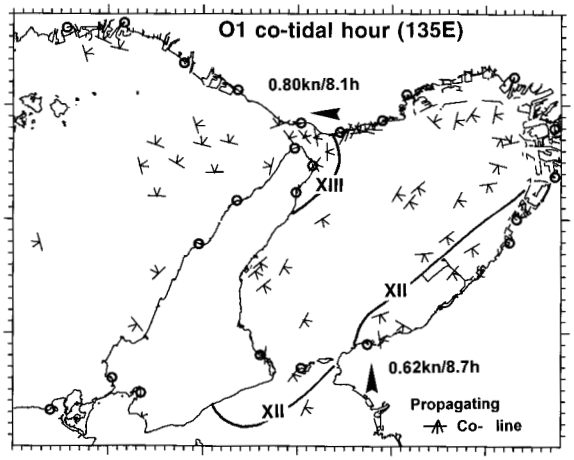

Fig. 5(b) Co-tidal charts for O_1.

4. 3 K_1 tide

As shown in Fig. 4(a), contrary to those of semidiurnal tides M_2 and S_2, K_1 tidal amplitude increases gradually from the south of Tomogashima-strait 24 cm to the inner area of Osaka Bay 26 cm and to Harima-nada 27cm. In Tomogashima-strait and Osaka Bay, K_1 tidal amplitude at the right-hand side of propagating direction looks slightly larger than at the left-hand side.

K_1 co-tidal lines show propagation from Kii-channel to the inner area of Osaka Bay in Fig. 4(b), which are also not so varied compared to those of semidiurnal tides. In Akashi-strait, its propagation is slowed, but it takes only about 1 hour (15 degrees) for passing. In Osaka Bay, co-tidal hour at the right-hand side advances slightly to that at the left-hand side.

4. 4 O_1 tide

O_1 tidal amplitude also increases gradually from the south of Tomogashima-strait 18cm to Harima-nada 20cm, and is almost same in that area. O_1 co-tidal hours are not so varied compared to that of the same diurnal tide K_1. In Osaka Bay, co-tidal hour in its southeastern coast is slightly earlier than that around Akasi-strait.

4. 5 Shallow water tides

In Osaka Bay, tidal curve is modified to irregular shape by shallow water tides. As shown in Table 1, shallow water tides such as fourth, third and sixth diurnal tides are developed more than 1cm in the innermost area. Major tides such as M_2 are reduced there as described above, so shallow water tides become noticeable for tidal prediction.

M_4 tidal amplitudes are 1.3-1.5 cm and their phase lags 30-50 degrees around the innermost of Osaka Bay. M_4 tide is further developed adjacent to Akashi-strait, and its amplitude reaches 5cm and 7.6cm in Esaki and Iwaya of Awaji-shima respectively. This M_4 development will be discussed in the later section.

Sixth-diurnal tides are also developed around the innermost of Osaka Bay. Particularly amplitude of $2MS_6$ reaches 2cm and phase lag is about 250-268 degrees there. Third-diurnal tides, compound tides of semidiurnal and diurnal tides, are also developed, where amplitudes of MK_3 and MO_3 are amplified to near 2cm.

5. Discussion

5. 1 Influence of earth rotation on tides and tidal currents in the narrow strait

Akashi-strait.

As shown in Fig. 2(a), co-amplitude line of 15cm encircles around the northern corner of Awaji-shima, where M_2 amplitude is smaller than surroundings. Fig. 6 shows schematic distribution of M_2 tidal harmonic constants around Akashi-strait. M_2 amplitude at Akashi is about 2.5cm larger than that at Esaki, and M_2 phase lags are almost same at both place. M_2 amplitude at Maiko is about 7cm larger than that at Iwaya. Thus it is reconginzed that amplitude along northern coast of the strait is apparently larger than that along southern coast.

In order to investigate characteristics of M_2 tidal wave, each term of momentum equation (2) is evaluated and listed in Table 2 as absolute value. Along major axis, the pressure gradient (c) is almost balanced with the time variable term (a), and along minor axis the pressure term (c) with the Coriolis term (b). Thereby, tidal current of major axis is recognized to behave as an oscillation along the strait. Tidal current of minor axis is so weak that pressure gradient (c) is geostrophically

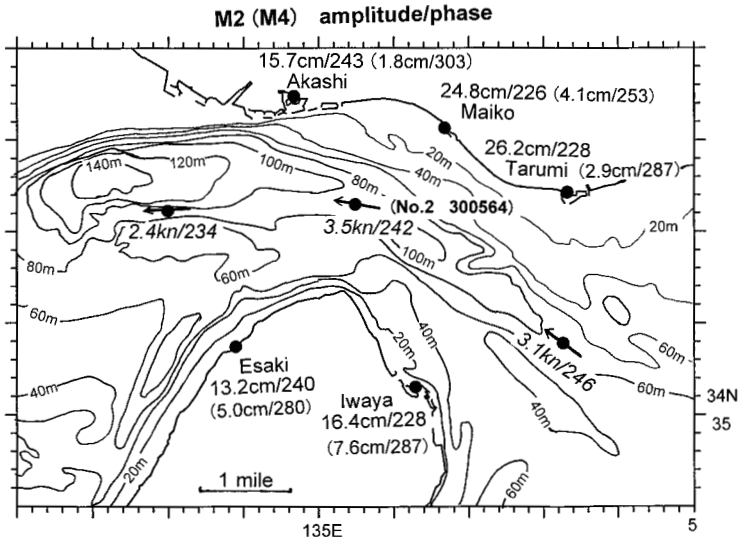

Fig. 6 Tidal Harmonic Constants Distribution of M_2 in Akashi-strait. Dot in the coast indicates the location of tide station and dot with arrow in the off coast indicates that of tidal current station. Numerals in brackets are those for M_4 tide. Numerals in the center of the strait are tidal current harmonic constants of M_2.

balanced with Coriolis force (b). Then, across the strait, sea surface is inclined to the left-hand side of current direction in proportion to the current speed in the northern hemisphere. This type of wave is well known as a Kelvin wave. Further, as shown in Fig. 6 and Table 2, since the phase of M_2 tide is almost same as that of M_2 tidal current, maximum flood current flowing to west occurs in High water and sea surface inclines from north to south. Maximum ebb current flowing to east occurs in Low water and sea surface inclines from south to north. Thereby tidal amplitude is amplified in the northern coast and reduced in the southern coast as shown in Fig. 7(a). Assuming the width of the strait Δx=4km and averaged current speed u=2kn as about half of the strongest current at the center of the strait, the difference of sea levels Δh between at the northern and southern coasts becomes 3.5cm according to geostrophic balance $\Delta h = f \cdot u \cdot \Delta x / g$. This value agrees fairly well with the observed differences of 2.5cm between Akashi and Esaki, or 7cm between Maiko and Iwaya in Fig. 6. Further the estimated arrows of gradients in the strait of Fig. 2(a) also confirm this tendency. Therefore distributions of co-amplitude lines and co-tidal lines shown in Fig. 2(a) and 2(b) respectively are well explained by the influence of earth rotation.

For S_2, tidal current is 25 degrees delayed to that of tide. Then flood current becomes in maximum after High water, and makes high water continued and co-tidal hour delayed in the northern coast of the strait. Therefore S_2 co-tidal lines are shifted to west in the northern coast as shown Fig. 3(b). Concerned to this shift, S_2 nodal area is located in the western coast of Awaji-shima as shown Fig. 3(a). Thus the location of S_2 nodal area are distinctively different from that of M_2 tide. This difference of S_2 and M_2 is considered due to the tidal response difference of the whole Seto Inland Sea to various tidal periods input, which is suspected particularly sensitive around Akashi-strait to semidiurnal tides. Tidal response of the whole Seto Inland Sea is remained for further investigation.

For diurnal tides, K_1 and O_1, their periods

Table 2 Tidal Current Harmonic Constants and Evaluation of terms of equation of motion in Akashi- and Tomogashima-straits.

Place	***Akashi Strait No.2 300564*** 34°37'12"N, 135° 0'42"E Depth 100m f=0.829 10^{-4} /s Layer= 5m	***Tomogashima-Strait 300150*** 34°16'18"N 134°59'36"E Depth 80m f=0.821 10^{-4}/s Layer=5m
M2	Sg=1.41 10^{-4}/s N 1.38kn(245) E 3.23kn(61) Major 293° 1.81m/s(242) 0.020 Minor 203° 0.04m/s(152) Tide 15.0cm(240) V.G 0.167 Dir 51 K.G 1.689 Dir 294 L (a) 2.54 (b) 0.03 (c) 2.60 (d) 0.69 S (a) 0.05 (b) 1.50 (c) 1.44 (d) 0.01	Sg=1.41 10^{-4}/s N 1.89kn(206) E 0.04kn(206) Major 1° 0.97m/s(206) 0.000 Minor 270° 0.00m/s(116) Tide 36.0cm(191) V.G 0.100 Dir 129 K.G 0.361 Dir 11 L (a) 1.37 (b) 0.00 (c) 1.39 (d) 0.25 S (a) 0.00 (b) 0.80 (c) 0.80 (d) 0.00
S2	Sg=1.45 10^{-4}/s N 0.55kn(264) E 1.11kn(78) Major 296° 0.64m/s(259) 0.042 Minor 206° 0.03m/s(169) Tide 9.5cm(234) V.G 0.065 Dir 72 K.G 0.870 Dir 311 L (a) 0.93 (b) 0.02 (c) 0.91 (d) 0.09 S (a) 0.04 (b) 0.53 (c) 0.49 (d) 0.00	Sg=1.45 10^{-4}/s N 0.53kn(217) E 0.10kn(236) Major 10°0.28m/s(218) 0.058 Minor 280 0.02m/s(128) Tide 18.5cm(215) V.G 0.021 Dir 111 K.G 0.213 Dir 11 L (a) 0.40 (b) 0.01 (c) 0.39 (d) 0.02 S (a) 0.02 (b) 0.23 (c) 0.20 (d) 0.00
K1	Sg=0.73 10^{-4}/s N 0.58kn(138) E 0.94kn(329) Major 302° 0.56m/s(146) -0.085 Minor 212° 0.05m/s(236) Tide 25.0cm(217) V.G 0.045 Dir 324 K.G 0.211 Dir 235 L (a) 0.41 (b) 0.04 (c) 0.46 (d) 0.07 S (a) 0.03 (b) 0.47 (c) 0.50 (d) 0.01	Sg=0.73 10^{-4} /s N 0.70kn(141) E 0.06kn(262) Major 358° 0.36m/s(141) 0.067 Minor 88° 0.02m/s(231) Tide 24.0cm(204) V.G 0.024 Dir 30 K.G 0.122 Dir 297 L (a) 0.26 (b) 0.02 (c) 0.25 (d) 0.03 S (a) 0.02 (b) 0.30 (c) 0.28 (d) 0.00
O1	Sg=0.68 10^{-4}/s N 0.46kn(107) E 0.66kn(307) Major 304° 0.41m/s(121) -0.168 Minor 214° 0.07m/s(211) Tide 18.0cm(202) V.G 0.034 Dir 316 K.G 0.219 Dir 227 L (a) 0.27 (b) 0.06 (c) 0.33 (d) 0.04 S (a) 0.05 (b) 0.34 (c) 0.38 (d) 0.01	Sg=0.68 10^{-4}/s N 0.62kn(129) E 0.11kn(210) Major 2° 0.32m/s(130) 0.173 Minor 92° 0.06m/s(220) Tide 18.5cm(181) V.G 0.018 Dir 52 K.G 0.121 Dir 307 L (a) 0.22 (b) 0.05 (c) 0.17 (d) 0.03 S (a) 0.04 (b) 0.26 (c) 0.22 (d) 0.00

f: (10^{-4}/s)Coriolis coefficient, Sg: (10^{-4}radian/s), Angular speed of each tide.
N: North component's amplitude(knot) and phase lag(degree), E: East component's.
Major: major axis elements of tidal current ellipse, direction(degree), amplitude(m/s), phase lag(degree), amplitude ratio of minor/major in which positive means clockwise rotation and negative means counter-clockwise. Minor: same as Major except for minor axis ellement.
Tide: given tidal amplitude and phase lag for calculation of gradient of amplitude and phase lag.
V.G: maginitude (10^{-4} m/m, non-dimension) and direction (degree) of gradient of amplitude
K.G: magnitude (10^{-4} radian/m) and direction (degree) of gradient of tidal phase lag.
L: magnitudes ($10^{-4}ms^{-2}$) of (a)time change, (b)Coriolis force, (c)pressure gradient and (d)bottom stress terms of the equation (2) for major axis. See the section 3.
S: same as above explanation for L except for minor axis.

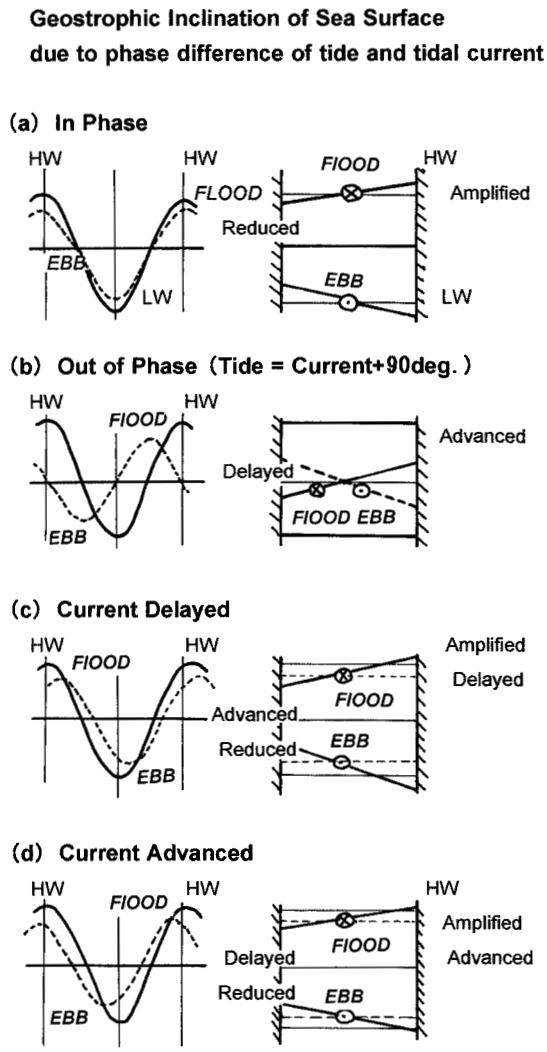

Fig. 7 Schematic diagram for geostraphic inclination. (a) Flood and ebb currents occur in phase with High and Low waters respectively. (b) Flood current occurs at mid time between High water and Low water. (c) Flood current occurs before High water. (d) Flood current occurs after High water.

are longer than inertia period 21.1 hours at the 34.6 degrees North, so that Coriolis term (b) to the time variable term (a) is expected to be more effective compared with the case of semidiurnal tide. As shown in Table 2, the term balance for diurnal tides suggests an oscillation along the strait and geostrophic inclination across the strait, too. But the phase difference of tide and tidal current is 71 degrees in K_1 and 81 degrees in O_1, which is large compared to those of semidiurnal tides. Then their currents are almost slack in their High water and Low water. Their maximum flood or ebb current occurs at the time of near mean water. Fig. 7(b) shows the conceptual relation of their tide and tidal current. Flood current tends to make tidal phase of High water advanced in the northern coast of the strait and delayed in the southern coast. Oppositely, ebb current tends to make tidal phase of Low water advanced in the northern coast and delayed in the southern coast. Therefore according to the influence of earth rotation, co-tidal hour is advanced in the northern coast and delayed in the southern coast, which is well agreed with Fig. 4(b) and 5(b).

Tomogashima-strait

M_2 tidal amplitude in the western coast of the strait is larger than that in the eastern coast as shown in Fig. 2(a), and M_2 co-tidal hour in the western coast advances to that in the eastern coast in Fig. 2(b). Major axis of tidal current directs to north. According to the term balances shown in Table 2, tidal current is considered to behave as an oscillation along the strait, and in geostrophic balance with surface elevation across the strait as same as that in Akashi-strait. But in Tomogashima-strait M_2 tidal current phase is delayed 15 degrees about 0.5 hour to M_2 tidal phase, while both phases are same in Akashi-strait. This means that maximum flood current direct to north occurs after High water and simultaneously sea surface inclines from east to west. Maximum ebb current direct to south occurs after Low water and simultaneously sea surface inclines from west to east. Therefore M_2 co-tidal hour is delayed in the eastern coast and advanced in the western coast according to this geostrophic

inclination. Fig. 7(c) explains this relation conceptually.

S_2 tidal current phase is almost same as its tidal phase, which is already explained in the case of Fig. 7(a). Therefore, S_2 amplitude increases in the eastern coast and decreases in the western coast, and its co-tidal hour is not so changed within the strait.

Co-tidal hours of K_1 and O_1 tidal currents are advanced about 4.2 and 3.4 hours (63 and 51 degrees) to those of K_1 and O_1 tides, respectively. Then maximum flood tidal currents occur some hours after their High water, and simultaneously sea surface is inclined east to west in order to balance with the Coriolis force, as shown in Fig. 7(d). Oppositely maximum ebb tidal currents occur some hours after their Low water, and sea surface is inclined west to east. Therefore, in the western coast, High and Low waters are postponed and reduced, and in the eastern coast they are set forward and amplified. These relations agree well with the amplitude and co-tidal hour distribution of Fig. 4(a), 4(b), 5(a) and 5(b) around the strait. Further, these relations of tide and tidal current are extended to the inner area of Osaka Bay, so that co-amplitude lines are drawn from NW to SE in Fig. 4(a) and 5(a) and co-tidal lines from NE to SW in Fig. 4(b) and 5(b).

5. 2 Generation of M_4 tide in Akashi-strait

Ogura(1933) already explained the M_4 generation and distribution due to the non-linear effect by tidal current. Its distribution and generation are discussed again here based on the recent tidal current data.

M_4 tidal amplitudes and phase lags are shown in Fig. 6, representing the values within the brackets. Its amplitudes at Iwaya and Esaki in the southern coast of the strait are 7.6 and 5.0cm, which are apparently larger than those at Akashi, Maiko and Tarumi in the northern coast, 1.8, 4.1 and 2.9cm, respectively. Its phase lags are from 253 to 303 degrees.

According to Ogura(1933), M_4 tide generation is concerned to two types of hydrodynamics. First is originated to the inertia term, sometimes called advection term. As mentioned above, maximum flood current and High water of M_2 tide occur simultaneously in Akashi-strait. Maximum ebb current and Low water occur simultaneously too. At High and Low waters, time change of sea surface is so little that the hydraulic equation of Bernoulli is applied assuming steady condition;

$$(7)\quad P_a/(\rho \cdot g) + H + v^2/2g = constant.$$

$P_a/(\rho \cdot g)$ means pressure head, H : elevation, and $v^2/2g$: velocity head. In here, P_a is atmospheric pressure, ρ : sea water density, v: current speed and g : gravity acceleration. Since atmospheric pressure is assumed almost same in the whole area, the equation (7) means that $H+v^2/2g$ is conserved along the stream. The elevation H is linear and the velocity head $v^2/2g$ is non-linear of quadratic. Then M_2 tidal current set in v can generate M_4 tide according to the non-linear effect of velocity head. Applying this relation to the M_2 tidal current in the center of Akashi-strait (1.81m/s, 242 degrees), the elevation H become;

$$\begin{aligned}(8)\quad H &= constant - v^2/2g \\ &= c. - (1.81 \cdot cos(\sigma t - 242))^2/2g \\ &= c. - 0.08\{cos(2\sigma t - 484) + 1\} \\ &= c. + 0.08\, cos(2\sigma t - 304) - 0.08 .\end{aligned}$$

Where, σ is the angular speed of M_2. Thereby M_4 tide is generated through (8), angular speed

is 2 σ, amplitude 8cm and phase lag 304 degrees. This estimated M_4 tide agrees well in order with the averaged distribution of M_4 as shown in Fig. 6.

Second, the difference of M_4 tide between in the northern coast and the southern coast of the strait is explained by the centrifugal force of the curved streamline. M_2 tidal current turns around the northern corner of Awaji-shima in both of flood and ebb. Water mass on the streamline is forced to outside by centrifugal force accompanied with this curved streamline. Then sea surface is expected to balance to this centrifugal force and to incline to the center of the curvature across the strait in both times of flood and ebb. This inclination occurs two times of flood and ebb during M_2 tidal current period, so that M_4 tide is generated. Assuming its radius R is 3 nautical miles and width of the strait L is 2 nautical miles as shown in Fig. 8, sea surface difference Δ between outside and inside is estimated from the balance of gravity and centrifugal forces in Fig. 8(b) as follows;

$$\Delta / L = v^2/gR$$

$$\Delta = v^2/gR \cdot L = (1.81 \cdot \cos(\sigma t - 242))^2/(9.8 \cdot 3) \cdot 2$$

$$= 0.11 \cdot \cos(2\sigma t - 124) \ .$$

In the times of flood and ebb, sea surface rises outside, and falls inside simultaneously. Then M_4 of amplitude 5cm and phase lag 124 degrees is induced outside (north) coast, and 5cm and 304 degrees inside (south) coast. Combined with the former M_4 component by the velocity head of M_2 tidal current, M_4 amplitude increases 13cm in the southern coast and decreases 3cm in the northern coast. These estimates are a little extreme but agree well with the tendency of M_4 tidal distribution in the strait in Fig. 6.

6. Summary and future subjects

Traditional co-tidal charts around Osaka Bay were drawn mainly based on the tidal harmonic constants. In this paper, gradients of tidal amplitude and co-tidal hour are evaluated based on the equation of motion using the tidal current harmonic constants. In results, co-tidal and co-amplitude charts have been improved and some distinctive features have been recognized as follows;

1. According to the concentration of M_2 co-tidal lines and the minimization of amplitude around the northern corner of Awaji-shima, a partial node of M_2 tide is recognized to shift to Awaji-shima and suspect-

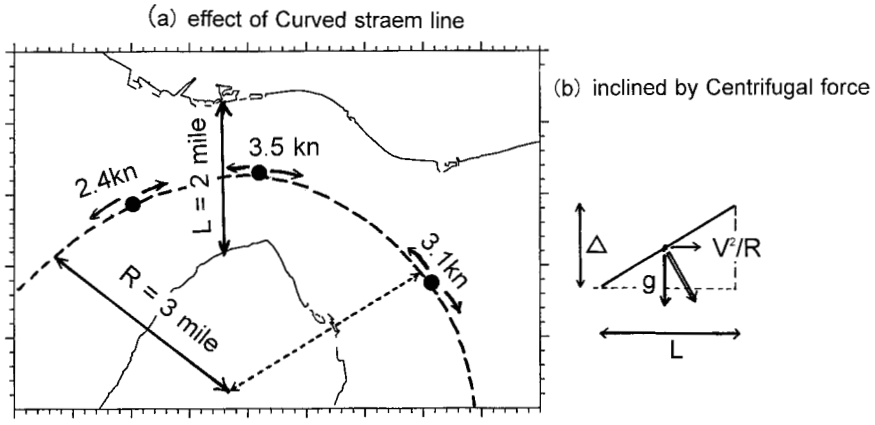

Fig. 8 Schematic diagram for the effect of curved streamline. (a) Assumed curvature of streamline, (b) Surface inclination by centrifugal force.

ed a virtual amphidrome like that in the Irish sea.

2. S_2 nodal area is recognized to shift to the western coast of Awaji-shima.
3. Diurnal tidal amplitudes of K_1 and O_1 tend to become large in the right-hand coast of propagation compared to that in the left-hand coast. Diurnal tidal phases tend to advance in the right-hand coast and delay in the left-hand coast.
4. Shallow water tides of fourth, sixth and third diurnal tides are developed in Osaka Bay. Particularly intensive development of M_4 tide occurs in Akashi-strait.

Through the analysis of tidal current and tide based on the equation of motion, it is concluded that tidal oscillation is controlled with the oscillating and the pressure terms along the strait, and with the Coriolis and the pressure terms across the strait. Therefore it is recognized that the locations of partial nodes depend on the mode distributions of individual tidal oscillations along the long axis of the Seto Inland Sea. Further, asymmetric distribution of tidal amplitude and phase lag in the charts across the strait is explained with this geostrphic control by Coriolis force, and the phase difference of tide and tidal current.

For the shallow water tide in Akashi-strait, it is concluded that M_4 tide is generated through the non-linear effect of velocity head from originated tides of M_2. Additionally, curved streamline induces the centrifugal force on water mass and makes the sea surface inclined across the strait in two times of flood and ebb. Thus tidal current in Akashi-strait can explain successfully the M_4 tide generation.

As mentioned above, principal characters of tides in Osaka Bay and surroundings are made clear and the improved co-tidal charts are proposed. But further investigation is necessary as follows;

a) Difference of nodal area of M_2 and S_2 indicates tide and tidal current distribution will be changed place to place by lunar condition. Other significant tides than M_2 and S_2 remain in this semidiurnal tidal band. Then tidal distributions for other semidiurnal tides and tidal change by lunar condition should be made clear.

b) Recently the change of tidal harmonic constants is pointed out and suspected due to the change of tidal response by geometric change of the sea such as land reclamation or dredging (Yoshida and Takasugi 2001). Then, since tidal distribution around Akashi-strait is sensitive as mentioned in this paper, its sensitivity should be investigated for such geometric change.

c) Around Akashi-strait, there are counter current eddy and strong current shear varied by place to place. Generation of M_4 tide is explained by tidal current distribution but its detail remains unknown. Then further tidal current observation and investigation are necessary to make fine tidal distribution.

Nowadays, various oceanographers and civil engineers try to make a numerical simulation model for tide and tidal current in the Seto Inland Sea, but its results are not often compared with actual co-tidal charts. Therefore author hopes this improved co-tidal charts to be utilized for such trial as validation.

Acknowledgement

Author thanks the reviewer for his critical reading and useful comments, and the staffs of Hydrographic Department JCG and 5th Regional JCG Hdqrs. for their efforts to collect

almost data used in this paper.

Data Sources

(1) Maritime Safety Agency : Tidal Harmonic Constant Tables Japanese coast, Pub. N0.742, 267p., (1992).

(2) Hiraiwa T., S. Saito, I. Fukuyama, N.Yoza, R. Goto, K. Ito and T. Kurokawa : Change of height of banch marks due to "the Hyogoken-nanbu Earthquake on January 17, 1995", Technical Bulletin on Hydrography 14, 111-118, (1996). (in Japanese)

(3) 5th Regional Maritime Safety Headquarters : Tidal Current Observation Report for Akashi-strait, (1995). (in Japanese)

References

Doodson, A. T. and H. D. Warburg : Admiralty Manual of Tides, *Hydrogr. Dep. Admiralty*, London, 270pp, (1941), reprinted in 1980.

Hendershott, M.C. and A. Speranza : Co-oscillating tides in long, narrow bays; the Taylor problem revisited, *Deep Sea Research*, **18**, 959-980, (1971).

Odamaki, M. : Tides and tidal currents in the Tusima Strait. *J. Oceanogr. Soc. Japan*, **45**, 65-82, (1989).

Ogura S. : The tides in the seas adjacent to Japan. *Bull. Hydrogr. Dept.*, **7**, 1-189, (1933a).

Ogura S. : On Tides and Tidal Currents in the north of Yellow Sea, *Suiro-Youhou* vol. **125**, 137-145, (1933b). (in Japanese)

Unoki S. : Coastal Physical Oceanography, 672pp, *Tokai Univ. Press*, (1993). (in Japanese)

Yashima K. : Some problems on the Sand Banks and Currents around Akashi Strait, *Technical Bulletin on Hydrography,* **10**, 79-89, (1992). (in Japanese)

Yoshida M. and Y. Takasugi : Tidal Variations due to Coastal Development in the Seto Inland Sea, - Inter-annual Change of Tide in the Last 30 Years -, *Umi-no-Kenkyu*, **10**, 123-135, (2001). (in Japanese)

大阪湾の同時潮図について
ーコリオリ力の影響ー

小田巻　実

要　約

潮流観測データに運動方程式を適用して潮汐振動特性を論じると共に同時潮図を精密に描きなおした．その結果，M_2振動の最小振幅の位置が淡路島北端側に偏っていることなどがわかった．この海域の潮汐分布には，コリオリ力の影響がかなり効いている．また，小倉（1933）が初めて論じた明石海峡のM_4分潮の発生についても，潮流観測データに基づき定量的に論じた．